A combined Speckle noise reduction and compression of SAR images using a multiwavelet based method to improve codec performance

J. Mvogo†, G. Mercier ††, V.P. Onana†, J.P. Rudant‡, E. Tonye†, H. Trebossen‡

†École Polytechnique de Yaoundé, Cameroun
†† École Nationale Supérieure des Télécommunications de Bretagne, Brest, France
‡Laboratoire de Géomatériaux - IFG - Université de Marne-La-Vallée, France

Abstract— **SAR images are corrupted by multiplicative noise (speckle) which limits the performance of the classical coder/decoder (codec) in the spatial domain. Our objective is to give an evaluation of the efficiency of a multiwavelet transform coding algorithm . We use the additional degree of freedom offered by multiwavelets to fine tune the number of vanishing moments and the approximation order of ours basis functions. Once the multiwavelet transform is performed, we apply an optimal bit allocation scheme on the subbands data using a set of Vector Quantizers. The quantization of the high frequencies multiwavelets coefficients may be though of as a hard thresholding algorithm. A measure of the equivalent number of looks is performed in the reconstructed SAR image in order to evaluate the impact of the codec in the noise reduction process.**

We compare our method with classical algorithm (baseline scalar wavelet transform followed by an optimal scalar quantization). The codec achieves comparable SNR, but performs surprising speckle noise reduction. Some results are presented with ERS-PRI images of Cameroon which can be compressed at $20:1$ while still remaining of sufficient quality for visual interpretation, segmentation and land use monitoring.

I. Introduction

In this paper a lossy compression scheme of SAR images based on the multiwavelet transform is evaluated. We investigate the reconstructed image quality using the SNR and the speckle reduction induced by the hard thresholding of the high frequencies during the quantization stage and the effects of the postfilter. We use a set of vector quantizers according to the vectorial output stream of the multiwavelet coefficients and the existence of fast quantizing and decoding algorithms [1]. In order to adjust the quantizers precision for each subband, a preliminary bit allocation scheme is performed. Section II presents a brief review on multiwavelet theory and mainly the multiwavelet transform algorithm. Section III describes the lossy compression algorithm based on optimal vector quantization of multiwavelet coefficients. Some experimental results are presented in Section IV.

II. The Multiwavelet Formalism

A. Scalar to vector wavelet

We mainly present here the multiwavelet theory which is a review of the scalar wavelets. It was shown in [2] that symmetry, orthogonality, compact support and approximation order $n > 1$ can be simultaneously achieved for multiwavelets.

A biorthogonal multiwavelet system consists of two multiscaling function vectors: $\boldsymbol{\phi} = [\phi_1, \phi_2, \ldots, \phi_r]^T$ and $\tilde{\boldsymbol{\phi}} = [\tilde{\phi}_1, \tilde{\phi}_2, \ldots, \tilde{\phi}_r]^T$ where $r > 1$ is an integer. The case $r = 1$ reduced the system to scalar wavelets. The multiscaling functions generate a multiresolution analysis pair consisting of $\{V_l\}_{l\in\mathbb{Z}}$ and $\{\tilde{V}_l\}_{l\in\mathbb{Z}}$ of $\mathcal{L}^2(\mathbb{R})^r$. $\boldsymbol{\phi}$ and $\tilde{\boldsymbol{\phi}}$ satisfy the refinement equations:

$$\boldsymbol{\phi}(\boldsymbol{x}) = \sum_k \boldsymbol{H}_k \boldsymbol{\phi}(2\boldsymbol{x} - k) \quad (1)$$

$$\tilde{\boldsymbol{\phi}}(\boldsymbol{x}) = \sum_k \tilde{\boldsymbol{H}}_k \tilde{\boldsymbol{\phi}}(2\boldsymbol{x} - k), \quad (2)$$

where $\{\boldsymbol{H}_k\}_{k\in\mathbb{Z}}$ and $\{\tilde{\boldsymbol{H}}_k\}_{k\in\mathbb{Z}}$ are finite length real-valued matrix sequences. We can associated to $\boldsymbol{\phi}$ and $\tilde{\boldsymbol{\phi}}$, the biorthogonal multiwavelets vectors: $\boldsymbol{\psi} = [\psi_1, \psi_2, \ldots, \psi_r]^T$ and $\tilde{\boldsymbol{\psi}} = [\tilde{\psi}_1, \tilde{\psi}_2, \ldots, \tilde{\psi}_r]^T$.

They are called multiwavelet functions. $\boldsymbol{\psi}$ and $\tilde{\boldsymbol{\psi}}$ satisfy the following equations:

$$\boldsymbol{\psi}(\boldsymbol{x}) = \sum_k \boldsymbol{G}_k \boldsymbol{\phi}(2\boldsymbol{x} - k), \quad (3)$$

$$\tilde{\boldsymbol{\psi}}(\boldsymbol{x}) = \sum_k \tilde{\boldsymbol{G}}_k \tilde{\boldsymbol{\phi}}(2\boldsymbol{x} - k), \quad (4)$$

where $\{\boldsymbol{G}_k\}_{k\in\mathbb{Z}}$ and $\{\tilde{\boldsymbol{G}}_k\}_{k\in\mathbb{Z}}$ are finite length real-valued matrix sequences.

The sequences $\{\boldsymbol{H}_k\}_{k\in\mathbb{Z}}$ and $\{\tilde{\boldsymbol{H}}_k\}_{k\in\mathbb{Z}}$ are called the matrix coefficients of lowpass multifilters whereas $\{\boldsymbol{G}_k\}_{k\in\mathbb{Z}}$ and $\{\tilde{\boldsymbol{G}}_k\}_{k\in\mathbb{Z}}$ constitute the corresponding matrix coefficients of highpass multifilters. The biorthogonal property of the multiscaling and multiwavelet functions implies the following relations:

$$\sum_{k\in\mathbb{Z}} \boldsymbol{H}_k \tilde{\boldsymbol{H}}_{k+2i}^T = 2\delta_i \boldsymbol{Id}, \quad (5)$$

$$\sum_{k\in\mathbb{Z}} \boldsymbol{H}_k \tilde{\boldsymbol{G}}_{k+2i}^T = 0, \quad (6)$$

$$\sum_{k\in\mathbb{Z}} \boldsymbol{G}_k \tilde{\boldsymbol{G}}_{k+2i}^T = 2\delta_i \boldsymbol{Id}, \quad (7)$$

where $\delta_i = 1$ if $i = 0$ and 0 otherwise in $\mathbb{Z}$.

B. Multiwavelet decomposition and reconstruction

This subsection describes the multiwavelet decomposition and reconstruction algorithms. One have to note that the Mallat multiresolution algorithm [3] for scalar wavelet can not be used directly for multiwavelet filters, the matrix-based coefficients requires a vectorial input signal. The problem of obtaining the vector input streams from a given signal is known as *prefiltering*. In this paper, we use the multiwavelets of multiplicity $r = 2$ and achieve presentation in one dimension.

Denote $\boldsymbol{\phi}_{l,k} = [\phi_{1,l,k}, \phi_{2,l,k}]^T$ and $\tilde{\boldsymbol{\phi}}_{l,k} = [\tilde{\phi}_{1,l,k}, \tilde{\phi}_{2,l,k}]^T$ the multiscaling functions. Likewise, we define $\boldsymbol{\psi}_{l,k}, \tilde{\boldsymbol{\psi}}_{l,k}$ the multiwavelet functions. Considering the multiresolution subspaces $\tilde{V}_l$ and $\tilde{V}_{l+1}$, we have for each $l \in \mathbb{Z}$: $\tilde{V}_l \subset \tilde{V}_{l+1}$ and $\overline{\bigcup_{l\in\mathbb{Z}} \tilde{V}_l} = \mathcal{L}^2(\mathbb{R})^r$.

Let consider now a vector signal $\boldsymbol{f} \in \tilde{V}_L \subset \mathcal{L}^2(\mathbb{R})^r$, then we have:

$$\boldsymbol{f}(\boldsymbol{x}) = \sum_{k\in\mathbb{Z}} \boldsymbol{P}_{L,k}^T \tilde{\boldsymbol{\phi}}_{L,K}(\boldsymbol{x}) \tag{8}$$

$$= \sum_{k\in\mathbb{Z}} \boldsymbol{P}_{L_0,k}^T \tilde{\boldsymbol{\phi}}_{L_0,k}(\boldsymbol{x}) + \sum_{l=L_0}^{L} \sum_{k\in\mathbb{Z}} \boldsymbol{Q}_{l,k}^T \tilde{\boldsymbol{\psi}}_{l,k}(\boldsymbol{x}), \tag{9}$$

where $L_0 < L$. $\boldsymbol{P}_{l,k}$ and $\boldsymbol{Q}_{l,k}$ are defined by:

$$\boldsymbol{P}_{l,k} = \int_{\mathbb{R}^r} \boldsymbol{f}(\boldsymbol{x})\boldsymbol{\phi}_{l,k}(\boldsymbol{x})d(\boldsymbol{x}) \tag{10}$$

$$\boldsymbol{Q}_{l,k} = \int_{\mathbb{R}^r} \boldsymbol{f}(\boldsymbol{x})\boldsymbol{\psi}_{l,k}(\boldsymbol{x})d(\boldsymbol{x}). \tag{11}$$

Using the refinement relation, for $L_0 < l \leqslant L$, we can deduce the following:

$$\begin{cases} \boldsymbol{P}_{l-1,k} = \sum_{m\in\mathbb{Z}} \boldsymbol{H}_{m-2k}\boldsymbol{P}_{l,m} \\ \boldsymbol{Q}_{l-1,k} = \sum_{m\in\mathbb{Z}} \boldsymbol{G}_{m-2k}\boldsymbol{P}_{l,m}. \end{cases} \tag{12}$$

These relations represent the decomposition algorithm. Conversely, the reconstruction algorithm is defined as ($L_0 < l \leqslant L$):

$$\boldsymbol{P}_{l,k} = \sum_{m\in\mathbb{Z}} \tilde{\boldsymbol{H}}_{k-2m}^T \boldsymbol{P}_{l-1,m} + \sum_{m\in\mathbb{Z}} \tilde{\boldsymbol{G}}_{k-2m}^T \boldsymbol{Q}_{l-1,m}. \tag{13}$$

The multiwavelet filter bank uses a vectorial input stream $\boldsymbol{f}$ from a given one dimensional input signal f. In out case, $r = 2$ and $\boldsymbol{f}$ is issued from $[f_{2k}, f_{2k+1}]^T$ multiplied by the prefilter matrix $\boldsymbol{\mathcal{P}}$.

III. Optimal bit allocation scheme

A. Allocation procedure

The codec is assigned to a target rate R_t, let us define r_j, d_j the rate and the distortion associated to the coding of multiwavelet coefficients for the subband j. The global distortion D and the global rate R are given by:

$$D = \sum_j d_j \quad \text{and} \quad R = \sum_j r_j, \tag{14}$$

where the d_j are evaluated with the MSE and the r_j with first order entropy.

The objective of the allocation scheme is to distribute the r_j between subbands in such a way that the distorsion D reaches the minimum while maintening the constraint $R \leqslant R_t$. We can formally write:

$$\min D = \min \sum_j d_j \quad \text{while} \quad R = \sum_j r_j \leqslant R_t. \tag{15}$$

In this paper, we consider a set of N vector quantizers. Let M be the total number of the multiwavelet subbands. For the i^{th} quantizer and the j^{th} subband we have the distorsion $d_{j,i}$ obtained from the rate $r_{j,i}$. We choose for each multiwavelet subband an optimal quantizer q_j^* in such a way that we minimize the global distortion:

$$D = \frac{1}{M}\sum_{j=1}^{M} d_{j,i}, \tag{16}$$

while maintaining the constraint:

$$R = \frac{1}{M}\sum_{j=1}^{M} r_{j,i} \leqslant R_t. \tag{17}$$

Some minimization algorithms for this type of problems have been introduced in [4]. To solve this problem, we use the lagrangian multiplier rule:

$$\min(D + \lambda R) = \min_{q_{j,i}}(\sum_{j=1}^{M} d_{j,i} + \lambda \sum_{j=1}^{M} r_{j,i}). \tag{18}$$

We describe succinctly the allocation algorithm:

1. Perform the multiwavelet transform of the SAR image with L levels of decomposition. Multiwavelet coefficients are denoted $W_{i,j}$.
2. For each subband j, evaluate the rate/distortion curve for the whole set of vectors quantizers Q. $R_{q\in Q}(j)$ and $D_{q\in Q}(j)$ denote the corresponding rates and distortions.
3. Allocate a value of λ.
4. For each subband j, determine the minimum of the Lagrangian function:

$$q_j^*(\lambda) = \arg\min_{q\in Q}[D_q(j) + \lambda R_q(j)], \tag{19}$$

to obtain the corresponding rate $R_{q_j^*(\lambda)}(j)$.

5. Compute the current rate: $R(\lambda) = \sum_{j=1}^{M} R_{q_j^*(\lambda)}(j)$;

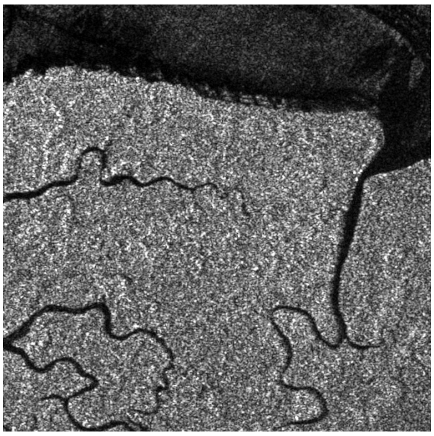

Fig. 1. Original ERS PRI image of Douala (Cameroun) ©ESA.

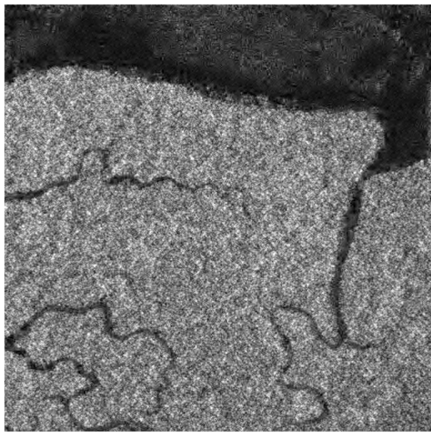

Fig. 2. Multiwavelet-based VQ at $\eta = 21 : 1$.

6. iterate 3,4 and 5 for a sequence of parameters λ until the optimum λ^* which corresponds to the target rate is reached.

In general, by using this algorithm, we obtain the target rate R_t or a very close value. In this later case, we use the steepest gradient slope procedure to adjust the precision of quantization in order to obtain the exact value R_t.

B. Vector quantization

Allocation procedure is applyied on the multiwavelet coefficients that are quantized by vectors of size 4. In fact, the vectorialization of the input using a prefilter along the lines and columns of the image give rise to vectors of size $2 \times r$ for the multiwavelet coefficients vectors (here $r = 2$). A set of multiresolution codebooks were generated with Kohonen's Self-Organizing Map Algorithm, with a variable learning rate [1].

IV. Experimental results

The codec is tested using a three looks ERS-PRI SAR image 512×512 of Douala from Cameroon (see Fig. 1). The multiwavelet transform used for the simulation is a three scale pyramid using an orthogonal cardinal balanced multiwavelet [5] and the identity prefilter and postfilter. The reconstructed SAR image shown in Fig. 2 has a compression ratio of $\eta = 21 : 1$. We further investigate two different aspects of the codec, the reconstruction error using the SNR and the speckle noise reduction obtained by calculating the equivalent number of looks L_{eq} on a homogeneous area. We compare the performance of our codec to the baseline scalar wavelet codec for various compression ratios using the two criteria SNR and L_{eq} (Tab. I).

It appears that optimal scalar quantization of scalar wavelet coefficients gives a better SNR. But taking into consideration the equivalent number of looks (L_{eq}), vector quantization of multiwavelet coefficients appears to yield a smoother image in a sense of an increase of homogeneity. It is understood that no artifact induced by the quantization is appalling for image interpretation.

V. Conclusion

Two optimal quantization techniques were compare to compress intensity SAR data: a wavelet-based scalar quantization and a multiwavelet-based vector quantization. The result suggests that the use of multiwavelets yields smart SAR image compression in the way of an equivalent number of looks improvement. The design of mother multifilters with higher degree of approximation and higher regularity may improve compression performances.

Acknowledgments

The authors would like to thank ESA for generous offer of ERS images that made this study possible, and the *Agence Universitaire de la Francophonie* for the support of our research.

References

[1] A. Czihò, B. Solaiman, G. Cazuguel, C. Roux, and I. Loványi, "Kohonen's self organizing feature maps with variable learning rate. Application to image compression," in 3rd *international workshop on Image and Signal Processing*, Santorini, Greece, 1997.

[2] V. Strela, P. Heller, G. Strang, P. Topiwala, and C. Heil, "The application of multiwavelet filter banks to image processing," *IEEE transactions on Image Processing*, vol. 8, no. 4, pp. 548–563, April 1999.

[3] S. Mallat, "A theory for multiresolution signal decomposition: the wavelet representation," *IEEE transactions on Pattern Analysis and Machine Intelligence*, vol. 11, pp. 674–693, 1989.

[4] Y. Shoham and A. Gersho, "Efficient bit allocation for an abitrary sets of quantizers," *IEEE Transactions on Acoustics, Speech and Signal Processing*, vol. 69, no. 9, pp. 1445–1453, September 1988.

[5] I. Selesnick, "Balanced multiwavelet bases based on symmetric FIR filters," *IEEE transactions on Signal Processing*, vol. 48, no. 1, pp. 184–191, January 2000.

TABLE I

Comparison of Scalar and Vector Quantizations according to the equivalent number of looks on homogeneous areas.

η	11 : 1	16.8 : 1	21 : 1	28 : 1	31 : 1
SQ L_{eq}	2.17	2.26	2.39	2.56	2.58
VQ L_{eq}	2.95	3.28	3.86	5.66	8.85